Solid State Sciences 12 (2010) 685–690

Contents lists available at ScienceDirect

Solid State Sciences

journal homepage: www.elsevier.com/locate/ssscie

Spin dimer and mapping analyses of the magnetic properties of $VO(CH_3CO_2)_2$ and $VO(OCH_2CH_2O)$

Hyun-Joo Koo [a,*], Myung-Hwan Whangbo [b]

[a] Department of Chemistry and Research Institute of Basic Sciences, Kyung Hee University, Seoul 130-701, Republic of Korea
[b] Department of Chemistry, North Carolina State University, Raleigh, NC 27695-8204, USA

ARTICLE INFO

Article history:
Received 28 May 2008
Received in revised form
26 March 2009
Accepted 28 March 2009
Available online 9 April 2009

Keywords:
Spin exchange interaction
Spin dimer analysis
DFT calculations
Vanadyl acetate
Vanadyl glycolate

ABSTRACT

The spin exchange interactions of $VO(CH_3CO_2)_2$ and $VO(OCH_2CH_2O)$ were investigated by performing spin dimer analysis based on tight binding calculations and mapping analysis based on first principles density functional theory calculations. In agreement with experiment, both analyses show that the magnetic properties of $VO(CH_3CO_2)_2$ and $VO(OCH_2CH_2O)$ are best described by uniform antiferromagnetic one-dimensional chain and isolated antiferromagnetic dimer models, respectively. Our study shows that the nearest-neighbor spin exchange in the one-dimensional chains of VO_5 square pyramids in $VO(CH_3CO_2)_2$ is mediated by the C $2p_\pi$ orbital of the carboxylate group, and that the *cis* spin dimers of $VO(OCH_2CH_2O)$ provide strong antiferromagnetic spin exchange than do the *trans* spin dimers of $VO(OCH_2CH_2O)$.

© 2009 Elsevier Masson SAS. All rights reserved.

1. Introduction

Vanadyl acetate $VO(CH_3CO_2)_2$ and vanadyl glycolate $VO(OCH_2CH_2O)$, synthesized by solvothermal reactions of vanadium pentoxide and lithium hydroxide in acetic acid and ethylene glycol, respectively, are of potential interest as precursors to battery materials [1]. In both compounds the V^{4+} (d^1) ions form VO_5 square pyramids, but the connectivity of their VO_5 square pyramids is different. $VO(CH_3CO_2)_2$ has one-dimensional (1D) chains of VO_5 square pyramids in which every pair of adjacent VO_5 square pyramids is bridged by two acetate ions (Fig. 1a), and these 1D chains are well separated. $VO(OCH_2CH_2O)$ contains 1D chains of VO_5 square pyramids in which the VO_5 pyramids share their basal edges such that the apical oxygen atoms of adjacent VO_5 pyramids alternate the patterns of *cis* and *trans* arrangements (Fig. 1b), hence leading to *cis* and *trans* dimer units $(VO)_2O_6$, respectively, along the chains. In each VO_5 square pyramid the basal oxygen (O_{bs}) atoms of one unshared basal edge are provided by one glycolate ion. The magnetic susceptibility of $VO(CH_3CO_2)_2$ shows a broad maximum characteristic of a low dimensional antiferromagnet. Casey and Thackeray [2] fitted the magnetic susceptibility with an Ising uniform antiferromagnetic (AFM) 1D chain model to find the spin exchange parameter $J/k_B = -239$ K, while Weeks et al. [1] fitted the susceptibility with a Heisenberg uniform AFM 1D chain model to obtain $J/k_B = -215$ K from the relationship $k_BT_{max}/|J| \approx 0.641$ [3], where T_{max} is the temperature at which the susceptibility maximum occurs. The spin exchange is strong despite that the magnetic orbitals of adjacent V^{4+} ions are parallel to the basal planes of the pyramids (Fig. 2) and hence makes a δ-type overlap. It is of interest to find why the acetate bridges provide very effective spin exchange interactions. The magnetic susceptibility of $VO(OCH_2CH_2O)$ exhibits a spin-gapped behavior and is well reproduced by an isolated AFM dimer model with $J/k_B = -460$ K [1]. It is interesting to find which type of dimers, *cis* or *trans*, of the edge-sharing 1D chains are responsible for the isolated AFM dimer behavior of $VO(OCH_2CH_2O)$.

To confirm a spin lattice model used for interpreting the magnetic properties of a given magnetic system, it is necessary to evaluate its spin-exchange interactions on the basis of electronic structure calculations [4,5]. The spin exchange interactions of $VO(CH_3CO_2)_2$ and $VO(OCH_2CH_2O)$ are either superexchange (SE) [6] interactions involving V–O–V paths or super-superexchange (SSE) [4,5] interactions involving V–O···O–V paths. In the present work we evaluate these interactions to determine which spin exchange paths lead to the spin lattices of the two compounds used in interpreting their magnetic properties. Two methods were used for our study, namely, qualitative spin dimer analysis [4,5] based on extended Hückel tight binding (EHTB) calculations [7] and quantitative mapping analysis [4a,8–10], based on first principles density functional theory (DFT) electronic structure calculations.

* Corresponding author. Tel.: +82 2 961 0981; fax: +82 2 966 3701.
E-mail address: hjkoo@khu.ac.kr (H.-J. Koo).

1293-2558/$ – see front matter © 2009 Elsevier Masson SAS. All rights reserved.
doi:10.1016/j.solidstatesciences.2009.03.023

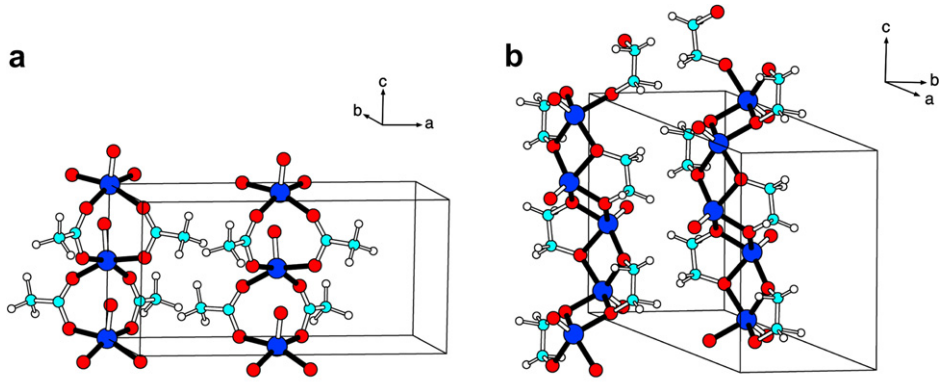

Fig. 1. (a) Perspective view of the crystal structure of $VO(CH_3CO_2)_2$, where the blue, red, cyan and white circles represent V, O, C and H atoms, respectively, the black cylinders represent the equatorial V–O_{bs} bonds of VO_5 square pyramid. (b) Perspective view of the crystal structure of $VO(OCH_2CH_2O)$, where the blue, red, cyan and white circles represent V, O, C and H atoms, respectively, and the black cylinders represent the equatorial V–O_{bs} bonds of VO_5 square pyramid (For interpretation of the references to colour in this figure legend, the reader is referred to the web version of this article.)

2. Quantitative mapping analysis

In mapping analysis based on first principles DFT electronic band structure calculations, the total energies of several ordered spin states of a given magnetic solid are calculated and then the energy differences between these states are related to the corresponding energy differences expected from the spin Hamiltonian,

$$\widehat{H} = -\sum_{i<j} J_{ij}\widehat{S}_i\widehat{S}_j,$$

where J_{ij} is the spin exchange parameter for the spin exchange interaction between the spin sites i and j, while $\widehat{S}_i$ and $\widehat{S}_j$ are the spin angular momentum operators at the spin sites i and j, respectively. If a spin dimer consists of two equivalent spin sites with N unpaired spins each, then the energies of the ferromagnetic (FM) and antiferromagnetic (AFM) states (i.e., the highest-spin and broken-symmetry states, respectively) of the spin dimer are given by $-N^2J/4$ and $N^2J/4$, respectively [11], so that the energy difference between the AFM and the FM states is equal to $N^2J/2$. Thus, the spin exchange parameter J is related to the electronic energy difference ΔE between the AFM and the FM states by $J = 2\Delta E/N^2$ [4a,11a,12,13].

For the 1D chain of $VO(CH_3CO_2)_2$ we consider the spin exchange interaction J_{nn} between nearest-neighbor V^{4+} ions. For the edge-sharing 1D chain of $VO(OCH_2CH_2O)$ we consider nearest-neighbor spin exchange interactions J_{cis} and J_{trans}, respectively, for the *cis* and *trans* dimers. J_{nn} can be determined by considering the two ordered spin sates, FM and AF, depicted in Fig. 3. For these states the total spin exchange energies per unit cell are written as (in the present case, $N = 1$) [11a,14],

$$E_{FM} = (-4J_{nn})\left(\frac{N^2}{4}\right), \tag{1a}$$

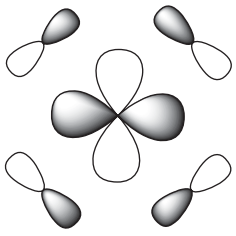

Fig. 2. Magnetic orbital of the V^{4+} ion in a VO_5 square pyramid.

$$E_{AF} = (4J_{nn})\left(\frac{N^2}{4}\right), \tag{1b}$$

from which we obtain,

$$J_{nn} = \left(\frac{1}{8}\right)\left(\frac{4}{N^2}\right)(E_{AF} - E_{FM}). \tag{1c}$$

J_{cis} and J_{trans} can be determined by considering the three ordered spin states FM, AF1 and AF2 as shown in Fig. 4. For these states the total spin exchange energies per unit cell are written as,

$$E_{FM} = (-4J_{cis} - 4J_{trans})\left(\frac{N^2}{4}\right), \tag{2a}$$

$$E_{AF1} = (4J_{cis} + 4J_{trans})\left(\frac{N^2}{4}\right), \tag{2b}$$

$$E_{AF2} = (4J_{cis} - 4J_{trans})\left(\frac{N^2}{4}\right), \tag{2c}$$

from which J_{cis} and J_{trans} can be expressed as follows:

$$J_{cis} = \left(\frac{1}{8}\right)\left(\frac{4}{N^2}\right)(E_{AF2} - E_{FM}), \tag{2d}$$

$$J_{trans} = \left(\frac{1}{8}\right)\left(\frac{4}{N^2}\right)(E_{AF1} - E_{AF2}). \tag{2e}$$

The total energies of the ordered spin states of $VO(CH_3CO_2)_2$ and $VO(OCH_2CH_2O)$ were calculated by performing spin-polarized DFT electronic band structure calculations with the projected augmented-wave method encoded in the Vienna ab initio simulation package [15]. Our calculations employed the generalized gradient approximation (GGA) for the exchange and correlation correction [16], the plane wave cut off energy of 450 eV, the on-site repulsion U on vanadium, and the sampling of the irreducible Brillouin zone with 144 k-points. To see how the value of U affects our results, we performed GGA plus onsite repulsion (GGA + U) calculations with $U = 4.5$ and 5.5 eV.

The spin exchange parameters calculated from the mapping analysis are summarized in Table 1. The spin exchange J_{nn} of $VO(CH_3CO_2)_2$ is calculated to be strongly AFM leading to a uniform

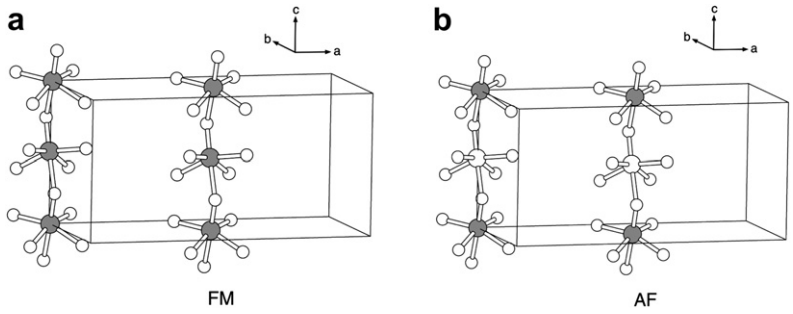

Fig. 3. Ordered spin arrangements (a) FM and (b) AF of $VO(CH_3CO_2)_2$, where the gray and white circles refer to the up and down spin sites of V atoms, respectively.

AFM 1D chain model, as found experimentally [1]. For $VO(OCH_2CH_2O)$, J_{cis} is strongly AFM while J_{trans} is weakly FM, which supports the use of an isolated AFM dimer model for $VO(OCH_2CH_2O)$ [1] and identifies the *cis* spin dimers as the units leading to the AFM dimers. Note that J_{cis} is calculated to be stronger than J_{nn} by a factor of approximately three, consistent with experiment (Table 1) [1]. For $VO(CH_3CO_2)_2$, the calculated spin exchange parameter J_{nn} (i.e., −293 K with $U = 4.5$ eV, −203 K with $U = 5.5$ eV) is in reasonable agreement with the experimental value (i.e., −219 K[1], −239 K[2]). For $VO(OCH_2CH_2O)$, the calculated J_{cis} (i.e., −891 K with $U = 4.5$ eV, −706 K with $U = 5.5$ eV) is larger than the experimental value (i.e., −460 K[1]) by a factor of about two.

Thus, the quantitative mapping analysis provides results consistent with experiment, namely, the magnetic properties of $VO(CH_3CO_2)_2$ and $VO(OCH_2CH_2O)$ are best described by uniform AFM 1D chain and isolated AFM dimer models, respectively, with strong AFM spin exchange, and identifies the *cis* dimers as the AFM dimer units in $VO(OCH_2CH_2O)$. However, this analysis does not provide a chemical picture as to why these are the cases. To explore this question, we perform qualitative spin dimer analysis in the next section.

3. Qualitative spin dimer analysis

The spin exchange parameter J between two spin sites can be written as $J = J_F + J_{AF}$, where J_F is the FM term ($J_F > 0$) and J_{AF} is the AFM term ($J_{AF} < 0$) [17]. When J_{AF} is very small in magnitude, the J_F term can dominate to make the overall spin exchange FM. In cases of strong AFM interactions, the trends in the J values are well approximated by those in the corresponding J_{AF} values [4,5], which for spin dimers with one spin at each spin site are described by[4,17]

$$J_{AF} \approx -\frac{(\Delta e)^2}{U_{eff}}. \quad (3)$$

Here the effective on-site repulsion U_{eff} is essentially a constant for a given compound, and Δe is the energy difference between the two magnetic orbitals representing the spin dimer when the two spin sites are equivalent. In the present work, the $(\Delta e)^2$ values are evaluated by performing EHTB calculations [7] for the spin dimers of $VO(CH_3CO_2)_2$ and $VO(OCH_2CH_2O)$.

The spin dimer for J_{nn} is given by $(VO)_2O_8$ if only the first-coordinate ligand atoms O_{bs} of the V^{4+} ions are used to define the spin dimer, but by $(VO)_2(O_2CCH_3)_6$ if it is taken into consideration that the O_{bs} atoms belong to the acetate ions $[CH_3CO_2]^-$. The *cis* and *trans* spin dimers of $VO(OCH_2CH_2O)$ are represented by $(VO)_2O_6$ if only the first-coordinate ligand atoms O_{bs} of the V^{4+} ions are used to define the spin dimer, but by $(VO)_2(OCH_2CH_2O)_4$ if we consider that the O_{bs} atoms are part of the glycolate ions $[OCH_2CH_2O]^{2-}$.

In our calculations of the $(\Delta e)^2$ values both the d orbitals of V and the s/p orbitals of its surrounding ligands were represented by double-zeta Slater-type orbitals (DZ-STO) [18], because such calculations are known to provide results consistent with experiment [4,5]. The radial part of a DZ-STO is expressed as

$$r^{n-1}[c_1\exp(-\zeta_1 r) + c_2\exp(-\zeta_2 r)],$$

where n is the principal quantum number, and the exponents ζ_1 and ζ_2 describe contracted and diffuse STOs, respectively (i.e., $\zeta_1 > \zeta_2$). The diffuse STO provides an orbital tail that enhances overlap between O atoms in the O···O contacts of the SSE paths V–O···O–V. The $(\Delta e)^2$ values are affected most sensitively by the exponent ζ_2 of the diffuse O 2 p orbital. To assess how the diffuseness of the O 2 p orbital affects the relative strengths of the SSE interactions, we replace ζ_2 with $(1 + x)\,\zeta_2$ and calculate the $(\Delta e)^2$ values for $x = 0.00$, 0.05 and 0.10. The atomic parameters used in our calculations are summarized in Table S1 (see the supporting information). To examine how the bridging ligands, $[CH_3CO_2]^-$ and $[C_2H_4O_2]^{2-}$, affect the spin exchange interactions, the $(\Delta e)^2$ values were calculated by including the $[CH_3CO_2]^-$ and $[C_2H_4O_2]^{2-}$ groups

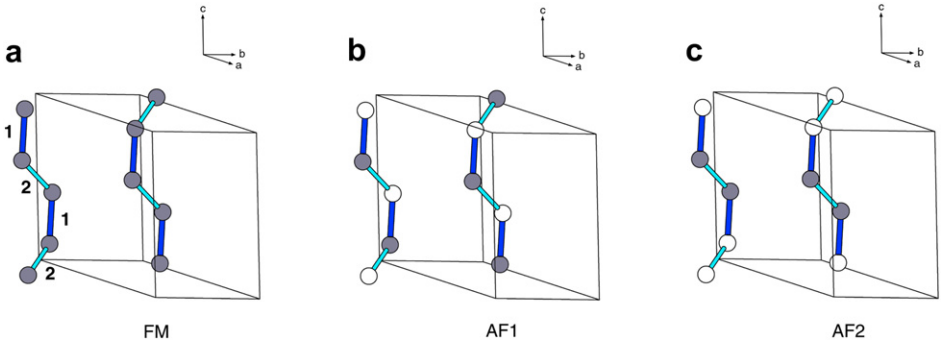

Fig. 4. Ordered spin arrangements (a) FM, (b) AF1 and (c) AF2 of $VO(OCH_2CH_2O)$, where the gray and white circles refer to the up and down spin sites of V atoms, respectively. The numbers 1 and 2 represent the spin exchange paths J_{cis} and J_{trans}, respectively.

Table 1
Calculated and experimental spin exchange parameters J (in k_BK) of $VO(CH_3CO_2)_2$ and $VO(OCH_2CH_2O$.

Compound	Parameter	Calculated J		Experimental J
		$U = 4.5$ eV	$U = 5.5$ eV	
$VO(CH_3CO_2)_2$	J_{nn}	−293	−207	−215,[a] −239[b]
$VO(OCH_2CH_2O)$	J_{cis}	−891	−706	−460[a]
	J_{trans}	+74	+76	

[a] Taken from Ref. [1].
[b] Taken from Ref. [2].

Table 2
$(\Delta e)^2$ values in $(meV)^2$ calculated for the spin dimers of $(VO)(CH_3CO_2)_2$ and of $(VO)(OCH_2CH_2O)$.

(a) $(VO)(CH_3CO_2)_2$						
x	$(VO)_2O_8$			$(VO)_2(O_2CCH_3)_6$		
	0.00	0.05	0.10	0.00	0.05	0.10
J_{nn}	670	290	120	31,800	22,700	15,700
(b) $(VO)(OCH_2CH_2O)$						
x	$(VO)_2O_6$			$(VO)_2(OCH_2CH_2O)_4$		
	0.00	0.05	0.10	0.00	0.05	0.10
J_{cis}	16300	17,600	18,900	40,600	37,900	35,300
J_{trans}	7020	4830	3050	3	1	4

explicitly as part of the spin dimers and also by replacing them with their O_{bs} atoms. The $(\Delta e)^2$ values calculated for the spin dimers representing J_{nn}, J_{cis} and J_{trans} are summarized in Table 2.

Table 2a shows that J_{nn} is very weak when the spin dimer is represented by $(VO)_2O_8$, as expected from the fact that the basal planes of the two VO_5 square pyramids are almost parallel in the spin dimer. If the spin dimer is represented by $(VO)_2(O_2CCH_3)_6$, however, J_{nn} is strongly enhanced. The cause for this change can be seen from the orbitals, ψ_+ and ψ_-, of the spin dimer responsible for the energy split Δe. As shown in Fig. 5, the magnetic orbitals of the VO_5 square pyramids have in-phase and out-of-phase π-type interactions in ψ_+ and ψ_- through their oxygen p-orbital tails, respectively. The C $2p_\pi$ orbital of the carboxylate carbon combines in-phase in ψ_+ to lower the energy, while it cannot interact with ψ_- by symmetry thereby increasing the energy split Δe between ψ_+ and ψ_-. In other words, the strong AFM spin exchange J_{nn} of

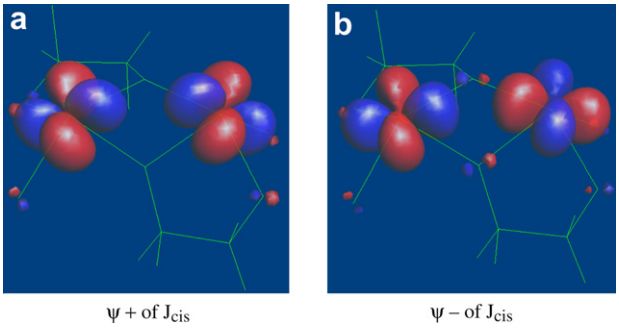

Fig. 6. Magnetic orbitals ψ_+ and ψ_- of the *cis* spin dimer $(VO)_2(OCH_2CH_2O)_4$ representing the spin exchange J_{cis} of $(VO)(OCH_2CH_2O)$.

$(VO)(CH_3CO_2)_2$ is provided by the C $2p_\pi$ orbital of the carboxylate group of $[CH_3CO_2]^-$.

For $VO(OCH_2CH_2O)$, Table 2b shows that J_{cis} is stronger than J_{trans} by a factor of 2–6 when the spin dimers are represented by $(VO)_2O_6$. When the spin dimers are represented by $(VO)_2(OCH_2CH_2O)_4$, however, J_{cis} is strengthened while J_{trans} becomes negligible, so that the spin lattice of $VO(OCH_2CH_2O)$ becomes an isolated AFM dimer model, which is in agreement with experiment. To understand why the *cis* and *trans* spin dimers are strongly different in their spin exchange interactions, we examine their magnetic orbitals ψ_+ and ψ_-. In both ψ_+ and ψ_-, the magnetic orbital planes of the two spin sites are not parallel for the *cis* spin dimer (Fig. 6) but parallel for the *trans* spin dimer (Fig. 7). As a consequence, the direct overlap between the xy orbitals of the V^{4+} ions across the shared edge is strong for the *cis* spin dimer, but weak for the *trans* spin dimer. A similar observation has been made for the *cis* and *trans* spin dimers found in vanadyl hydrogen phosphate $VO(HPO_4)\cdot 0.5H_2O$ [5].

In the *cis* and *trans* spin dimers of $VO(OCH_2CH_2O)$, the dihedral angle θ between the basal planes of the two edge-sharing VO_5 square pyramids (Fig. 8) is significantly different, namely, $\theta = 141.4°$ for the *cis* spin dimer and $\theta = 175.6°$ for the *trans* spin dimer. To see whether or not the large difference between J_{cis} and J_{trans} is related to this difference in θ, we first construct the idealized structures of *cis*- and *trans*-V_2O_8 spin dimers (Fig. 8) by using the average V–O_{bs} and V–O_{ap} (here O_{ap} refers to the apical O atom of the VO_5 square pyramid) bond lengths as well as the average $\angle O_{ap}$–V–O_{bs} bond angle taken from the experimental crystal structure of $VO(OCH_2CH_2O)$ (i.e., V–O_{ap} = 1.577 Å, V–O_{bs} = 2.007 Å and 1.934 Å, and

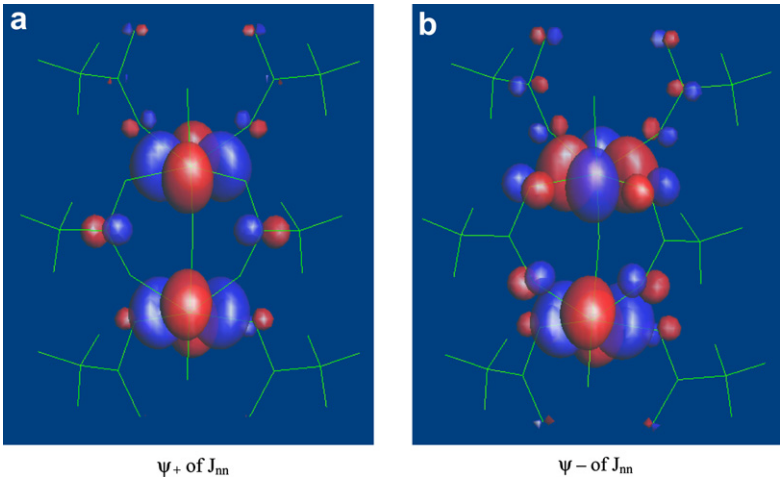

Fig. 5. Magnetic orbitals ψ_+ and ψ_- of the spin dimer $(VO)_2(O_2CCH_3)_6$ representing the spin exchange J_{nn} of $VO(CH_3CO_2)_2$.

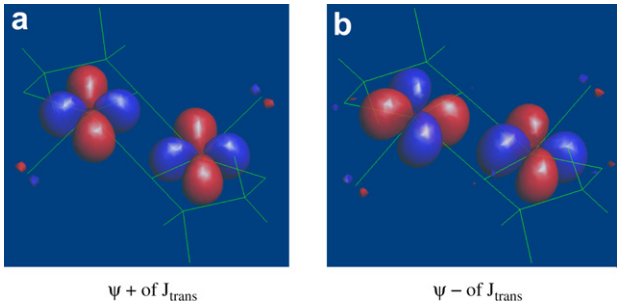

Fig. 7. Magnetic orbitals ψ_+ and ψ_- of the *trans* spin dimer $(VO)_2(OCH_2CH_2O)_4$ representing the spin exchange J_{trans} of $(VO)(OCH_2CH_2O)$.

$\angle O_{ap}–V–O_{bs} = 112.9°$Å). We then calculate the $(\Delta e)^2$ values of the *cis*- and *trans*-V_2O_8 spin dimers as a function of the dihedral angle θ. Table 3 summarizes the $(\Delta e)^2$ values as well as the V···V distances as a function of θ. Note that $(\Delta e)^2$ is much greater for the *cis* dimer than for the *trans* dimer for all values of θ between 140° and 180°. The difference in the dihedral angles θ of the *cis* and *trans* spin dimers is not responsible for the large difference between J_{cis} and J_{trans}. The V···V distance of the *cis* dimer for $\theta = 140°$ is shorter than that of the *trans* dimer for $\theta = 175°$ (i.e., 2.991 vs. 3.045 Å). This enables the *cis* spin dimer to have a stronger AFM spin exchange through the direct overlap between the xy orbitals of its V^{4+} ions than does the *trans* spin dimer. However, it is noted from Table 3 that the *cis* dimer has a much larger $(\Delta e)^2$ value than does the *trans* dimer even when the *cis* dimer has a longer V···V distance. For the spin exchange between adjacent V^{4+} ions in the edge-sharing VO_5 pyramids, the mirror-plane symmetry of the *cis* dimer is much more effective than is the inversion symmetry of the *trans* dimer. This is due to the overlap between the xy orbitals of adjacent V^{4+} ions as well as the overlap of the xy orbitals of the V^{4+} ions with the 2p orbitals of the bridging O_{bs} atoms.

4. Discussion and concluding remarks

The first-principle evaluation of the spin exchange parameters of a crystalline solid can be carried out either in terms of electronic band structure calculations for various ordered spin states of the solid, as described in Section 2, or in terms of cluster electronic structure calculations for various isolated spin dimer units [4,9]. The cluster-calculation approach involves negatively charged spin dimers so that the spin exchange parameters resulting from cluster calculations can be incorrect. For instance, the spin exchange parameters of Li_2CuO_2 obtained from the embedded cluster calculations [19] differ from those obtained from the band-calculation approach [20]. It is the spin exchange parameters from the band-calculation approach that correctly explain the magnetic properties of Li_2CuO_2 [20]. Thus, we have not attempted to do first principle cluster calculations for $VO(CH_3CO_2)_2$ and $VO(OCH_2CH_2O)$ to extract their spin exchange parameters. The spin dimer analysis based on the EHTB method, though based on cluster calculations, is unaffected by charges since the EHTB method is a one-electron method.

Both the quantitative mapping and qualitative spin dimer analyses show that the magnetic properties of $VO(CH_3CO_2)_2$ and $VO(OCH_2CH_2O)$ are best described by uniform AFM 1D chain and isolated AFM dimer models, respectively, in agreement with experiment, and the *cis* dimers are the AFM dimer units in $VO(OCH_2CH_2O)$. The spin dimer analysis reveals that the strong AFM spin exchange J_{nn} of $(VO)(CH_3CO_2)_2$ is mediated by the C $2p_\pi$ orbital of the carboxylate group of $[CH_3CO_2]^-$. In $VO(OCH_2CH_2O)$, the *cis* spin dimer has a much stronger AFM spin exchange than does the *trans* spin dimers, which shows that, for the spin exchange between adjacent V^{4+} ions in the edge-sharing VO_5 pyramids, the mirror-plane symmetry of the *cis* dimer is much more effective than is the inversion symmetry of the *trans* dimer. Our work points out that a combined approach of quantitative mapping and qualitative spin dimer analyses is useful in attaining quantitative and qualitative understanding of magnetic properties.

Table 3
Values of the V···V distance in Å and $(\Delta e)^2$ in $(meV)^2$ calculated for the idealized *cis*-V_2O_8 and *trans*-V_2O_8 spin dimers as a function of the dihedral angle θ between the basal planes of the two edge-sharing VO_5 square pyramids.[a]

θ (Degree)	*cis*-V_2O_8		*trans*-V_2O_8	
	V···V	$(\Delta e)^2$	V···V	$(\Delta e)^2$
180	2.615	2,83,500	3.045	4170
175	2.680	2,19,600	3.042	4160
170	2.741	1,69,300	3.033	4100
165	2.796	1,29,200	3.019	4010
160	2.846	97,400	2.998	3890
150	2.929	52,600	2.741	3650
140	2.991	25,600	2.861	3680

[a] The experimental dihedral angles for the *cis*- and *trans*-V_2O_8 dimers are 141.4° and 175.6°, respectively.

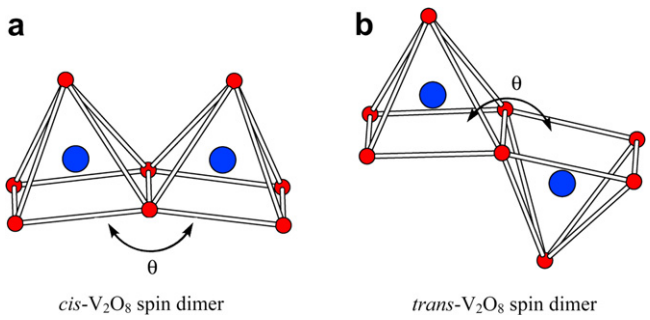

Fig. 8. Schematic representations of the idealized (a) *cis*-V_2O_8 spin dimer and (b) *trans*-V_2O_8 spin dimer, where θ represents the dihedral angle between the basal planes of the two edge-sharing VO_5 square pyramids.

Acknowledgements

The work at Kyung Hee University was supported by the Korean Research Foundation Grant KRF-2007-C00028 funded by the Korean Government (MOEHRD, Basic Research Promotion Fund), and at North Carolina State University by the Office of Basic Energy Sciences, Division of Materials Sciences, U.S. Department of Energy, under Grant DE-FG02-86ER45259.

Appendix. Supporting information

Supporting information associated with this article can be found in the online version, at doi: 10.1016/j.solidstatesciences.2009.03.023.

References

[1] C. Weeks, Y. Song, M. Suzuki, N.A. Chernova, P.Y. Zavalij, M.S. Whittingham, J. Mater. Chem. 13 (2003) 1420.
[2] A.T. Casey, J.R. Thackeray, Aust. J. Chem. 22 (1969) 2549.
[3] O. Kahn, Molecular Magnetism, VCH Publishers, Weinheim, Germany, 1993.
[4] (a) For reviews, see: M.H. Whangbo, H.J. Koo, D. Dai J. Solid State Chem. 176 (2003) 417;
(b) M.H. Whangbo, D. Dai, H.J. Koo, Solid State Sci. 7 (2005) 827.
[5] (a) H.J. Koo, M.H. Whangbo, Inorg. Chem. 40 (2001) 2169;
(b) H.J. Koo, M.H. Whangbo, P.D. VerNooy, C.C. Torardi, W.J. Marshall, Inorg. Chem. 41 (2002) 4664;
(c) M.H. Whangbo, H.J. Koo, D. Dai, D. Jung, Inorg. Chem. 42 (2003) 3898;
(d) H.J. Koo, M.H. Whangbo, K.S. Lee, Inorg. Chem. 42 (2003) 5932;
(e) H.J. Koo, D. Dai, M.H. Whangbo, Inorg. Chem. 44 (2005) 4359;
(f) H.J. Koo, M.H. Kang, Solid State Sci. 9 (2007) 955.

[6] J.B. Goodenough, Magnetism and the Chemical Bond, Wiley, Cambridge, MA, 1963.
[7] (a) R. Hoffmann, J. Chem. Phys. 39 (1963) 1397;
(b) Our calculations were carried out by employing the SAMOA (Structure and Molecular Orbital Analyzer) program package (This program can be downloaded free of charge from the website Available from: http://chvamw.chem.ncsu.edu/.
[8] L. Noodleman, J. Chem. Phys. 74 (1981) 5737.
[9] F. Illas, I. de P.R. Moreira, C. de Graaf, V. Barone, Theor. Chem. Acc. 104 (2000) 265 and the references cited therein.
[10] (a) A. Chartier, P. D'Arco, R. Dovesi, V.R. Saunders, Phys. Rev. B 60 (1999) 14042 and the references cited therein;
(b) D. Dai, M.H. Whangbo, H.J. Koo, X. Rocquefelte, S. Jobic, A. Villesuzanne, Inorg. Chem. 44 (2005) 2407;
(c) H.J. Koo, M.H. Whangbo, Inorg. Chem. 47 (2008) 128;
(d) H.J. Koo, M.H. Whangbo, J. Solid State Chem. 181 (2008) 276.
[11] (a) D. Dai, M.H. Whangbo, J. Chem. Phys. 114 (2001) 2887;
(b) D. Dai, M.H. Whangbo, J. Köhler, C. Hoch, A. Villesuzanne, Chem. Mater 18 (2006) 3281.
[12] D. Dai, H.J. Koo, M.H. Whangbo, J. Solid State Chem. 175 (2003) 341.
[13] (a) R. Grau-Crespo, N.H. de Leeuw, C.R. Catlow, J. Mater. Chem. 13 (2003) 2848;
(b) C. Loose, E. Ruiz, B. Kersting, J. Kortus, Chem. Phys. Lett. 452 (2008) 38.
[14 D. Dai, M.H. Whangbo, J. Chem. Phys. 118 (2003) 29.
[15] (a) G. Kresse, J. Hafner, Phys. Rev. B 62 (1993) 558;
(b) G. Kresse, J. Furthmüller, Comput. Mater. Sci. 6 (1996) 15;
(c) G. Kresse, J. Furthmüller, J. Phys. Rev. B 54 (1996) 11169.
[16] J.P. Perdew, K. Burke, M. Ernzerhof, Phys. Rev. Lett. 77 (1996) 3865.
[17] P.J. Hay, J.C. Thibeault, R. Hoffmann, J. Am. Chem. Soc. 97 (1975) 4884.
[18] E. Clementi, C. Roetti, Atomic data nuclear data tables 14 (1974) 177.
[19] C. de Graaf, I. de P.R. Moreira, F. Illas, Ó. Iglesias, A. Labarta, Phys. Rev. B 66 (2002) 014448.
[20] H.J. Xiang, C. Lee, M.H. Whangbo, Phys. Rev. B 76 (2007) 220411 (R).